Application of Dielectric Relaxation Spectroscopy to Ultrathin Langmuir−Blodgett Films

Toemsak Srikhirin,[†,⊥] Donald E. Schuele,[‡] J. Adin Mann, Jr.,[§] and Jerome B. Lando*[,†]

Polymer Microdevice Laboratory, Department of Macromolecular Science, Physics Department, and Chemical Engineering Department, Case Western Reserve University, Cleveland, Ohio 44106

Received August 23, 1999

ABSTRACT: The dynamic properties of ultrathin Langmuir−Blodgett (LB) films of side chain liquid crystalline copolymers were studied by dielectric relaxation spectroscopy (DRS). The technique is sensitive in detecting relaxation phenomena and transitions of these multilayers. The activation energy (E_a) of what we designate as the β-relaxation in copolymers with different spacer length, copolymer composition, and chromophore was measured. Incorporating the nitrobiphenyl (NBP) group in the side chain causes a disruption of the packing which resulted in a reduction in the activation energy of the β-relaxation. The substitution of a nitrostilbene group (NSB) for NBP and methoxy biphenyl (OMe) for a methoxy ethoxy methoxy biphenyl (MEMBP) resulted in a change in the relaxation spectra which is related to the difference in the packing of the multilayer films. The dielectric loss over the entire frequency range of the copolymer with shorter spacers showed similar behavior in the high-frequency region as the long spacer. An anomalous peak in the capacitance and dielectric loss was observed around room temperature.

Introduction

There is considerable interest in thin-film technologies, e.g., optical applications, as well as properties of ultrathin polymeric films.[1−5] The Langmuir−Blodgett (LB) technique is one method of fabricating ultrathin films with a well-defined thickness and molecular orientation. A complete understanding of the properties of films prepared by the LB technique is often limited by the characterization techniques that can be applied to these films. These limitations are mainly caused by the thickness of the LB sample. There are several techniques that have been successfully applied for LB film characterization:[1−6] among them FTIR, UV−vis, contact angle, AFM, SEM, X-ray, and electron diffraction. However, only a few techniques are capable of a dynamic study of the films, e.g., FTIR-ATR. This work deals with the application of dielectric spectroscopy to the study of the dynamics of LB films.

Dielectric spectroscopy is the study of the response of material to an applied electric field with special emphasis on the permanent dipoles. This technique has proven to be very useful in dynamic studies since it covers a wide frequency range of 10^{-4}−10^{9} Hz.[7−11] It also allows a direct observation of the dynamics of the thin film without introducing any probe species into the film. Moreover, this technique has also been proven to be a powerful tool for investigating molecular dynamics of both polymers and liquid crystalline polymers.[7−9,12−14]

Dielectric and electrical properties of metal/LB/metal films have been subjected to extensive study by several research groups. Jonscher et al.[11] applied dielectric spectroscopy to the study of stearic acid multilayers on a gold or aluminum substrate. The intrinsic voltage of Al/barium stearate/Al was also investigated by Singal et al.[15] Nonlinear dielectric properties of Al/calcium behenate/Al were investigated by Marc and Messier.[16] Some other materials—phospholipid[17] fatty acids, *o*-phenanthroline,[18] and stearic acid[19,20]—were also investigated.

Our objective is to apply dielectric spectroscopy to study the dynamics of side chain liquid crystalline copolymers having a noncentrosymmetric structure (Figure 1).

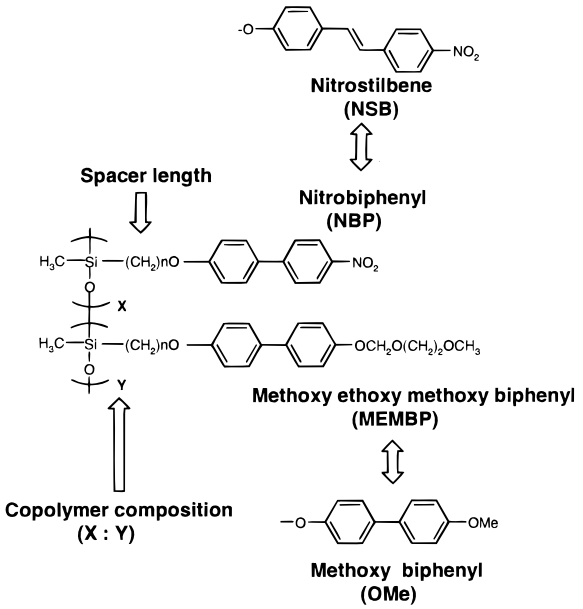

Figure 1. List of all materials that were used in this study.

Experiment

Glass slides from Corning (Corning, NY) were cleaned by boiling in a mixture of 30% hydrogen peroxide and 70% sulfuric

[†] Department of Macromolecular Science.
[‡] Physics Department.
[§] Chemical Engineering Department.
* To whom correspondence should be addressed.
[⊥] Present address: Max-Planck Institute for Polymer Research, Ackermannweg10, Mainz 55128, Germany.

10.1021/ma991437y CCC: $19.00
Published on Web 03/11/2000

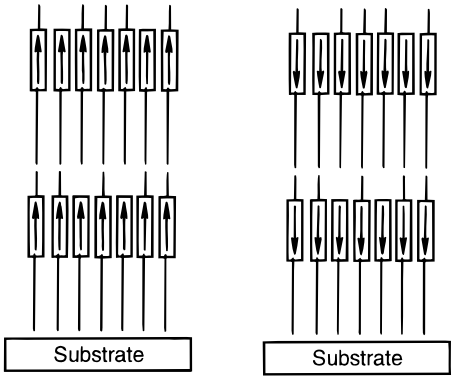

Figure 2. Picture illustrating the *x*- and *z*-type structures of the LB films.

acid at 90 °C for 1 h, rinsing with deionized water throughout, and drying with dry nitrogen. Aluminum electrodes were deposited onto the glass slide by evaporation using a Denton vacuum system, a DV-502 high-vacuum evaporator with DEG-2 power supply. The deposition pressure was 10^{-5} Torr. The aluminum wire, 1.5 mm in diameter, was obtained form Alfa AESAR (Ward Hill, MA) with 99.999% purity. The aluminum electrode is designed so that an electrical clip can be attached directly to the sample. The sample was heat sunk to the copper base of the temperature controller system with a silicone heat sink compound (CT40-a) from Chemtronics, Inc., Kennesaw, GA.

The measurements were carried out under a vacuum of 200−300 mmHg. The temperature was controlled by a Lake-Shore Cyrotronics DRC 82C temperature controller.

Dielectric loss (G/ω), where G is conductivity, and capacitance (C) were measured at 17 frequencies (10 Hz−100 kHz, in a linear log ratio) using a ratio arm transformer bridge at 1 K temperature interval. The high-precision three-terminal capacitance bridge used is the model CGA-83, C. Andeen and Associate, Cleveland, OH. The entire system is controlled by a personal computer operation over the IEEE 488 bus.

Curve fitting was performed using Igor Pro 3.1 (Wave Metrics, Inc., Lake Oswego, Oregon). No data will be reported for frequencies above $10^{3.5}$ Hz since they are dominated by the effective series resistance of the electrodes.

Materials. All the synthesis and characterization of the materials were reported in previous publications.[21−23] All the variations of the structure that were used in this study are shown in Figure 1. The annotation for copolymer will be referred to as "Cop", followed by the spacer length, copolymer composition, and the chromophore type. For example, Cop11/50% NBP is a copolymer with an 11-methylene spacer having a copolymer composition of 50% NBP and 50% MEMBP (Figure 1).

Sample Deposition. The aluminum-coated slide was cleaned with chloroform, dried in dry nitrogen, and kept in a desiccator saturated with hexamethyldisiloxane (HMDS) vapor for at least 24 h prior to deposition. Thus a hydrophobic surface was created.

The monolayer and multilayer deposition technique was a layer-by-layer horizontal deposition[21,22] (Figure 2).

Results and Discussions

The multilayer samples had a head-to-tail polar structure with a net dipole (Figure 2). X-ray diffraction indicated a noncentrosymmetric structure.[21−23] The layer thickness calculated from X-ray diffraction measurements is in agreement with the measurement from X-ray reflectivity.[22]

The dielectric measurement was done using a capacitance bridge, and the data were obtained as capacitance and loss (in picofarad, pF), which were converted

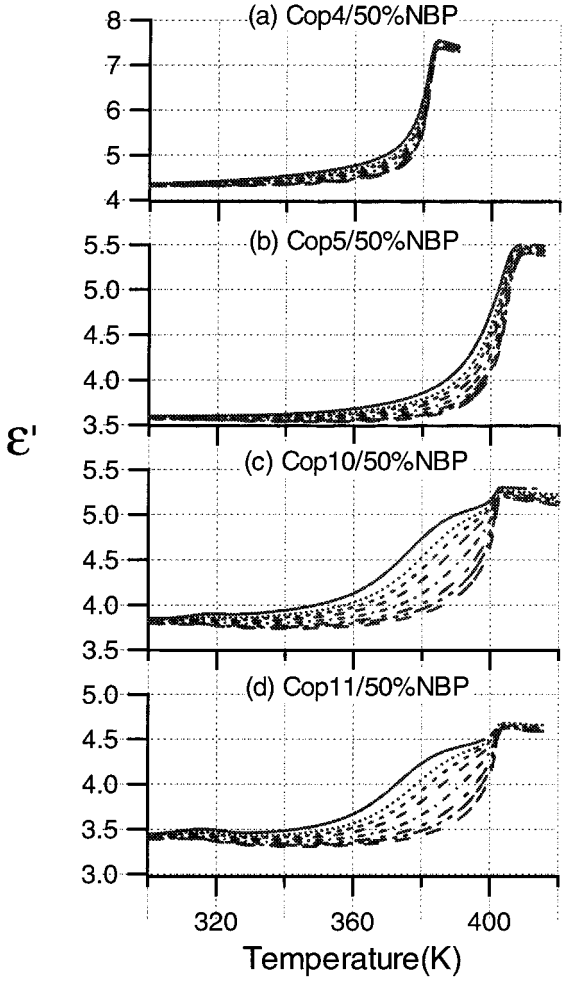

Figure 3. ϵ' of 15 layers of (a) Cop4/50% NBP, (b) Cop5/50% NBP, (c) Cop10/50% NBP, and (d) Cop11/50% NBP first run at (—)10, (• • •) 20, (- - -) 31.25, (- - •) 50, (- • -) 100, (— • —) 200, (—• • —) 312.5, and (— — —) 500 Hz.

to ϵ' and ϵ'' by the following equations

$$C = \frac{\epsilon_0 \epsilon' M}{\alpha} = \epsilon' C_0 \tag{1}$$

$$L = \frac{\epsilon_0 \epsilon'' M}{\alpha} = \epsilon'' C_0 \tag{2}$$

M is the area (in m^2), α is the sample thickness (in m), and ϵ_0 is the vacuum permittivity[10] where the sample geometry was unknown; a comparison was made by comparing the geometry-independent dissipation factor.

$$\tan \delta = \epsilon''/\epsilon' \tag{3}$$

It was observed that the capacitance and loss showed a lower value under vacuum compared to air. Backfilling with dry nitrogen or argon showed no change from the vacuum results. This difference was suspected to be an effect of the moisture in the air absorbed into the film. A similar observation was also reported in several metal/LB/metal samples.[16,17] Therefore, all the measurements were carried out after the sample was held under vacuum until there was no longer any measurable change (3 h) in the capacitance and loss.

The measurements were made in the direction of increasing temperature. A check on two samples showed

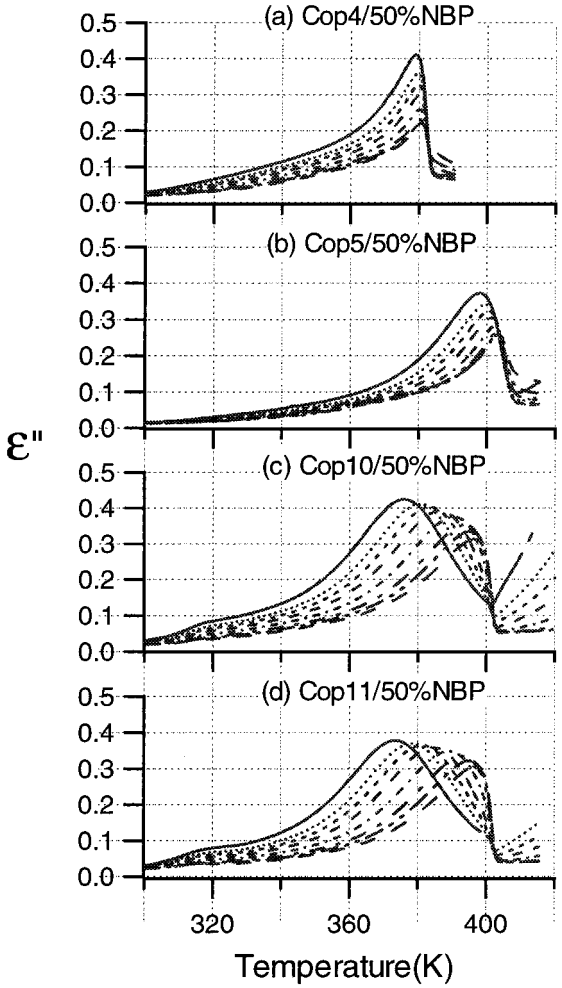

Figure 4. ϵ'' of 15 layers of (a) Cop4/50% NBP, (b) Cop5/50% NBP, (c) Cop10/650% NBP, and (d) Cop11/50% NBP first run at (—)10, (• • •) 20, (- - -) 31.25, (- - •) 50, (- • -) 100, (— • —) 200, (—• • —) 312.5, and (— — —) 500 Hz.

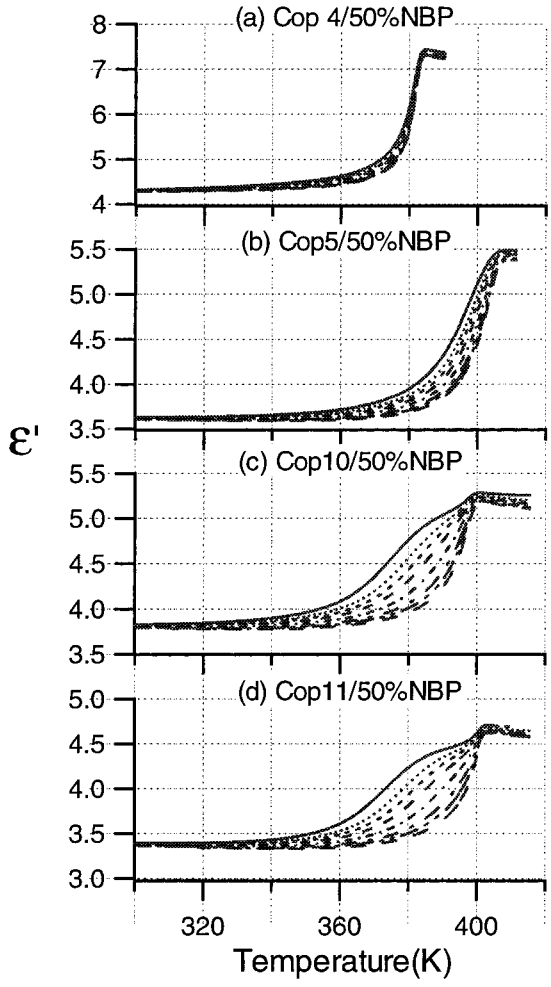

Figure 5. ϵ'' of 15 layers of (a) Cop4/50% NBP, (b) Cop5/50% NBP, (c) Cop10/50% NBP and (d) Cop11/50% NBP second run at (—)10, (• • •) 20, (- - -) 31.25, (- - •) 50, (- • -) 100, (— • —) 200, (—• • —) 312.5, and (— — —) 500 Hz.

no difference in the measured results between increasing and decreasing temperature runs in the K-phase.

To clarify the growth of aluminum oxide at high temperature, the aluminum coated on the glass slide was heated to 430 K and maintained at that temperature overnight. There was no significant change in the resistance of the aluminum. It was found that the aluminum did not further oxidize; however, if silver paint contacts were used, the sample tended to show a very high resistance once the sample was held at high temperatures for a few hours. This is because of the degradation of the binder within the silver paint. Contact with the aluminum electrode was made with a copper electrode.

This work will be focused on the effect of basic chemical structure—spacer length, composition, and chromophore type—on the dielectric response of the LB films.

Effect of Spacer Length. To examine the effect of spacer length, the copolymer compositions, MEMBP: NBP, were fixed at 1:1 (Figure 1). The temperature dependence of the dielectric response of Cop11/50% NBP, Cop10/50% NBP, Cop5/50% NBP, and Cop4/50% NBP at frequencies between 10 and 500 Hz is shown in Figures 3 and 5 for $\epsilon'(T)$ and Figures 4 and 6 for $\epsilon''(T)$.

$\epsilon'(T)$ and $\epsilon''(T)$ of Cop11/50% NBP and Cop10/50% NBP showed very similar behavior. Two processes were observed. The first process was observed as a small peak at around 310−320 K in both the real part, $\epsilon'(T)$, and the imaginary part, $\epsilon''(T)$. The peak amplitude decreased as the frequency increased and was not discernible at high frequencies. The origin of this process is still not known unequivocally, but there is evidence that it may be related to detrapping charge and/or structural rearrangement within the film. This peak will be referred to as the anomalous peak. This process was believed to be a morphological change since no peak is observed in the frequency plot in this temperature range. There is no change observed in the IR spectrum over this temperature range.[21] Both $\epsilon'(T)$ and $\epsilon''(T)$ peaks were observed in the same temperature range in a previous measurement by Nguyen.[22b] These peaks were not observed in shorter spacer length samples, Cop4/50% NBP and Cop5/50% NBP. The anomalous peak is no longer present after a thermal cycle to a temperature higher than 350 K.

The second loss peak, which we call a β-relaxation, was at higher temperature (Figures 3−6) and was frequency-dependent. Samples with different chain lengths responded differently. Thus, both $\epsilon'(T)$ and $\epsilon''(T)$ will be considered as a function of the side chain length. The $\epsilon'(T)$ of Cop10/50% NBP and Cop11/50% NBP at low frequency increased as the temperature increased and remained at a high value after the crystalline to liquid crystalline, K−LC, transition at 409 K which is

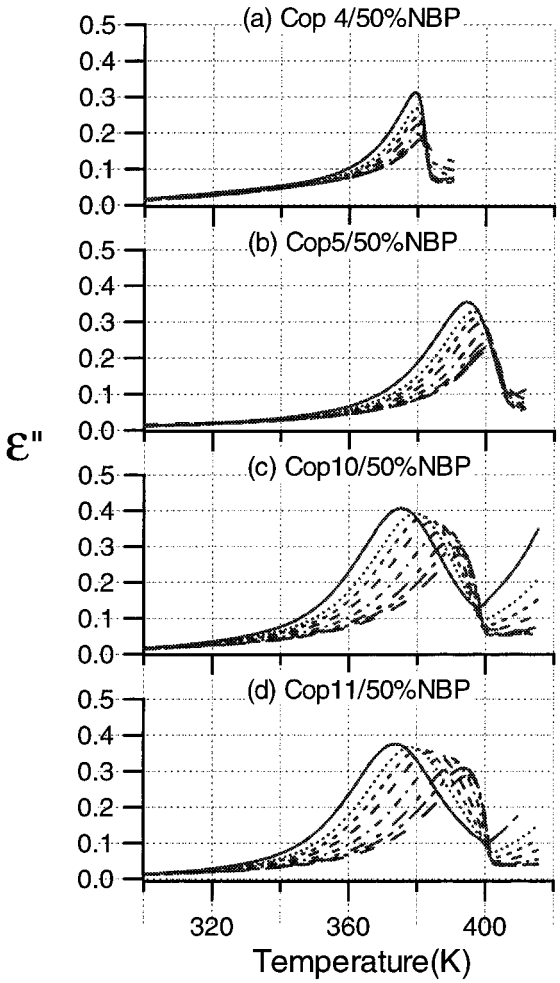

Figure 6. ϵ'' of 15 layers of (a) Cop4/50% NBP, (b) Cop5/50% NBP, (c) Cop10/50% NBP and (d) Cop11/50% NBP second run at (—)10, (• • •) 20, (- - -) 31.25, (- - •) 50, (- • -) 100, (— • —) 200, (—• • —) 312.5, and (— — —) 500 Hz.

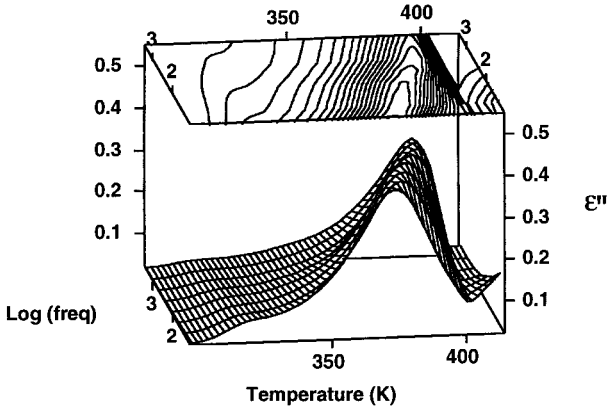

Figure 7. Three-dimensional plot of ϵ'' of Cop11/50% NBP (15 layers) first run.

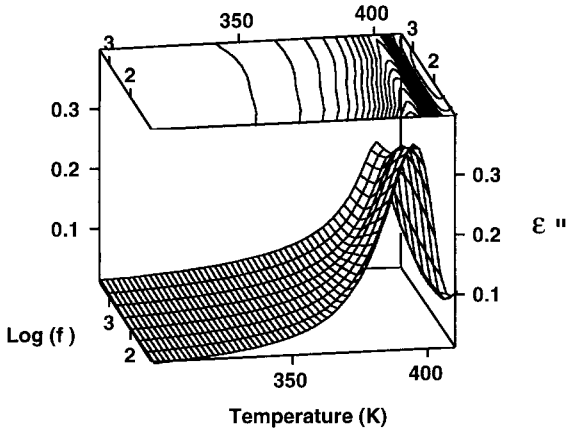

Figure 8. Three-dimensional of ϵ'' of Cop11/50% NBP (15 layers) first run.

somewhat higher than the broad β-relaxation. The process was also accompanied by a loss peak.

The contribution of the dipoles to the change in ϵ' in the higher frequency region took place in the neighborhood of the K−LC transition. $\epsilon''(T)$ approached the transition temperature as if hitting a wall since all the loss peaks fell off steeply at the transition temperature (Figures 4 and 6). The increase in $\epsilon'(T)$ is caused by an increase in the flexibility of the dipoles participating in the relaxation process while the $\epsilon''(T)$ represents the energy dissipation of that process. This means that at the low frequency the molecular dipoles have enough time to respond to the field; however, they cannot respond to the field at the high frequency. A movement of dipoles in the solid state has also been observed in several side chain liquid crystalline polymers.[24,25] These characteristics are easily observed in 3-dimensional plots (Figures 7 and 8) where the spanning and crossing of the β relaxation can be easily seen.

The shorter spacer length materials, Cop4/50% NBP and Cop5/50% NBP, behave in a more rigid manner than the longer spacer length materials, Cop10/50% NBP and Cop11/50% NBP. The dipoles appear to be quite rigid until the K−LC transition temperature is approached. The β-relaxation occurs over a shorter temperature range (Figures 3−8).

Another point is the fact that the response of the Cop4/50% NBP and Cop5/50% NBP at lower frequencies behaved somewhat similar to the response of the systems with longer spacer lengths at higher frequencies. It would be interesting to examine the shorter spacer length materials at a frequency lower than 10 Hz, the limit of the bridge.

To characterize the relaxation process, the frequency dependence needs to be considered. Both Cop10/50% NBP and Cop11/50% NBP behaved similarly in the frequency dependence plot. Only Cop11/50% NBP will be used as an example in data analysis. Figure 9 shows the typical decline in ϵ' as a function of frequency as the material goes through a relaxation peak as shown in Figure 10. The frequency dependence data contain other effects: dc conductivity and electrode resistance.

The loss peaks of copolymers in this study all share a common feature at high frequencies, $10^{3.5}$−10^5 Hz, where the electrode resistance begins to dominate. To simplify the data analysis, all the data beyond $10^{3.5}$ Hz were discarded to prevent an overcontribution of the electrode resistance to the curve-fitting procedure.

Curve Fitting. An overview of the fitting procedure which employs the Fuoss−Kirkwood (FK) function can be found in the publication of Akin[2] and Zhong.[27] The fitting parameters were chosen by examining the frequency dependence and temperature dependence plots. One relaxation process, the β-relaxation, is observed prior to the K−LC phase transition. The shape of the loss peak appears to be symmetrical in the frequency dependence plot; therefore, a relaxation process with a symmetrical loss peak was assumed for the fitting. The FK function is essentially a subset of a more general

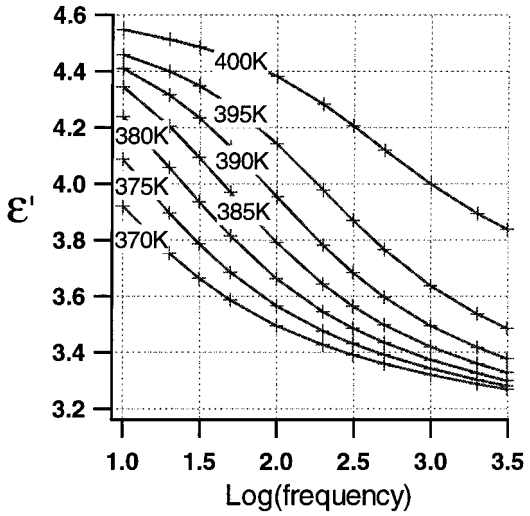

Figure 9. ϵ' of Cop11/50% NBP 15 layers at 370−400 K (first run).

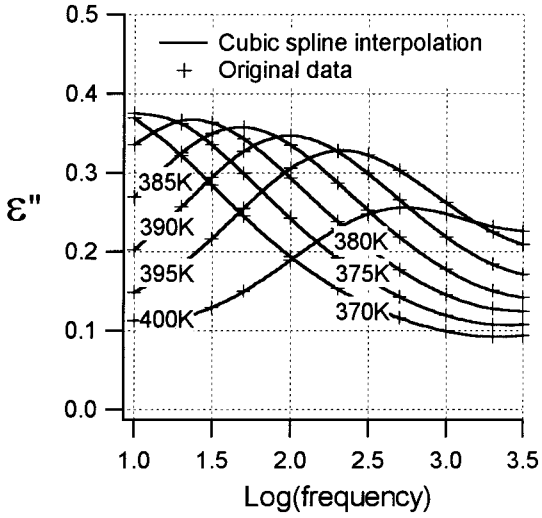

Figure 10. ϵ'' of Cop11/50% NBP 15 layers at 370−400 K (first run).

Havriliak−Negami (NH) function which takes into account an asymmetric relaxation peak.

The dc conductivity at low frequency and high temperature was taken into account by inserting a $1/\omega$ term in the FK function. The FK function has a symmetric empirical line shape and can be used to fit the data by means of a nonlinear least-squaresd minimization method.[28] The fitting function can be written for dc conductance, the relaxation term (FK), and the electrode resistance term in the form

$$\frac{G(\omega)}{\omega} = \frac{G_{dc}}{\omega} + A \sec h\left[\beta \ln\left(\frac{\omega}{\omega_R}\right)\right] + \omega \frac{C_p^2 R_S}{C_0} \quad (4)$$

with $\omega = 2\pi f$, the normalized loss spectra are

$$\epsilon'' = \frac{\sigma_{dc}}{2\pi f \epsilon_0} + \epsilon''_m \sec h\left[2.303\beta \log\left(\frac{f}{f_R}\right)\right] + f \frac{C_p^2 R_S}{C_0} \quad (5)$$

where A and ϵ''_m are the loss amplitude and the amplitude of the imaginary part of the complex dielectric constant. C_p is parallel capacitance.

There are five parameters in the fitting: dc conductivity (G_{dc}), peak amplitude (ϵ''_m), the width parameter (β), peak center (f_R), and electrode resistance (R_S). The frequency-dependent loss peaks increase in frequency as the temperature is increased. The fitting was done at every temperature by starting from the highest temperature where all the fitting parameters have a finite value. Also, it is to be noted that the dc conductivity is very low in these samples.

Table 1. Contribution from the Fitting of Cop11/50% NBP (15 Layers) First Run

T (K)	σ_{dc} (10^{-10} S/m)	ϵ''	β	log f_R
400.3	0.278	0.244	0.523	2.68
395.3	0.110	0.323	0.518	2.33
390.3	NA	0.344	0.494	2.00
385.3	NA	0.355	0.481	1.69

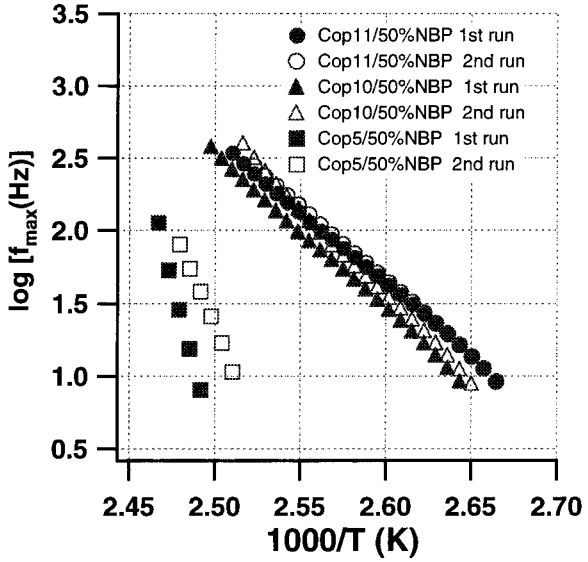

Figure 11. Plot of log[f_{max}(Hz)] vs 1000/T of Cop11/50% NBP, Cop10/50% NBP, and Cop5/50% NBP (15 layers) first and second run.

The fitted data for Cop11/50% NBP are shown in Table 1. The σ_{dc} is in the range of 2.78×10^{-12} S/m, which is small, indicating the high quality of the films. The plot of $\epsilon''(f)$ peak maximum, log f_R, and 1/temperature ($1/T$) is shown in Figure 11. The activation energy, E_a, was obtained from the slope of the Arrhenius plot.

$$\log f_{max} = \log B - \frac{E_a}{2.303RT} \quad (6)$$

and

$$E_a = \text{slope} \times 2.303R \quad (7)$$

where R is the gas constant. B represents an amplitude of the exponential dependence of f_{max}.

The calculated activation energies are shown in Table 2. The activation energy is lower for increased spacer length, indicating an increase in the flexibility of the dipoles. The difference in activation energy of the first run and the second run accompanies the disappearance of the low-temperature anomalous peak.

The subtraction between the first and the second run of Cop11/50% NBP is shown in Figure 12 where the anomalous peak can be clearly seen. Subsequent runs showed no change in the temperature characteristics of the data. The causes of the changed will be discussed later in this section.

Table 2. Activation Energy for the First and Second Run of the 15-Layer Sample

material	activation energy (kJ/mol) 1st run	2nd run
spacer length effect		
Cop4/50% NBP	NA[a]	NA
Cop5/50% NBP	360	
Cop10/50% NBP	211	234
Cop11/50% NBP	188	199
thickness effect of Cop11/50% NBP		
10 layers	209	214
15 layers	188	199
18 layers	180	194
composition effect		
Cop11/20% NBP	234	278
Cop11/63% NBP	178[b]	186[b]
chromophore effect		
Cop11/50% NSB	224	265
Cop11/50% OMe	162	174

[a] NA = the activation energy cannot be calculated. [b] Twelve-layer sample.

Table 3. List of the K−LC Transition of Cop System for First and Second Run by Dielectric Experiment

copolymer spacer	K−LC transition by dielectric experiment (K) 1st run	2nd run
spacer length effect		
Cop4/50% NBP	382.0	381.5
Cop5/50% NBP	404.0	403.0
Cop10/50% NBP	401.5	400.0
Cop11/50% NBP	401.5	401.0
thickness effect of Cop11/50% NBP		
10 layers	397.9	397.4
18 layers	391.1	391.1
composition effect		
Cop11/20% NBP	400.0	399.5
Cop11/63% NBP	401.0[a]	401.1[a]
spacer length effect		
Cop11/50% NSB	416.8	414.7
Cop11/50% OMe	413.2	414.2

[a] Twelve-layer sample.

The anomalous peak was not observed in the shorter spacer length, Cop4/50% NBP and Cop5/50% NBP. However, they also exhibited a higher temperature β-relaxation. The K−LC transition was slightly different between Cop4/50% NBP and Cop5/50% NBP due to an odd−even effect. The spread of the β-relaxation peak in the temperature plot was narrower in the Cop4/50% NBP, with no peaks in the frequency plot (10−500 Hz) for the Cop4/50% NBP. Thus, E_a could not be determined for this sample. The temperature spread of the β-relaxation in Cop5/50% NBP was greater than in Cop4/50% NBP but was still less than in Cop10/50% NBP and Cop11/50% NBP. In Cop5/50% NBP, the activation energy was 360.7 kJ/mol, which is higher than the longer spacer length.

The materials were different only in the length of the CH_2 units while the dipole groups of the materials were the same. Here, the nature of cooperative motions of the side chains may be different. The total change in magnitude of $\epsilon'(T)$ in the temperature dependence plot was smaller for the longer spacer length because of the volume effect, since ϵ' depends on the dipole moment per unit volume. Since the other parameters are the same, the molecule with the shorter spacer or smaller volume per molecule will possess a higher ϵ'.

This can be understood considering the following analogy. The molecule consists of two parts: the chromophore, E, and the methylene side chain, B. The molecular length of E is assumed to be constant, d_E, while the molecular length of B, d_B, depends on the side chain length. Both groups can be considered as a capacitance in series.

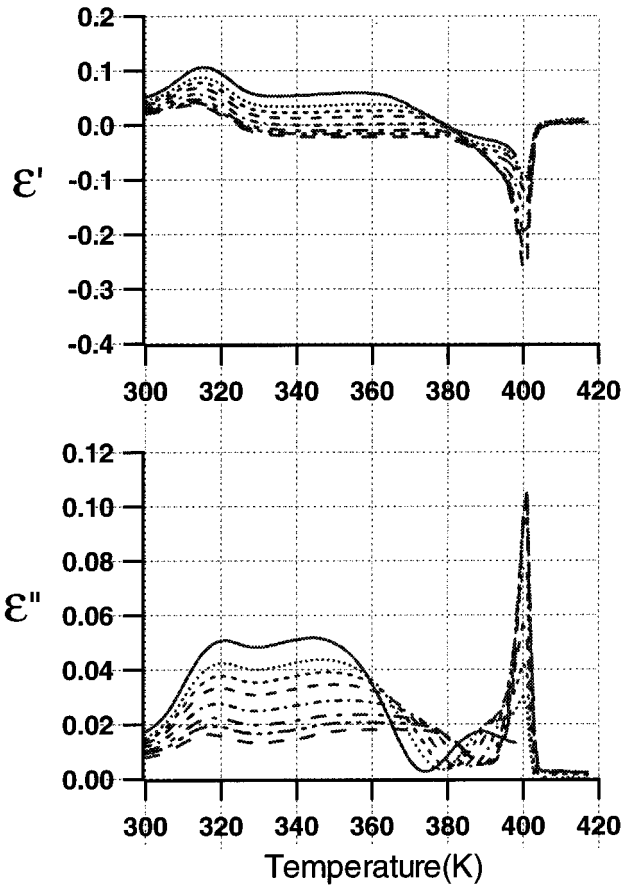

Figure 12. Difference between ϵ' and ϵ'' after subtraction of first and second run of Cop11/50% NBP 15 layers: (—)10, (• • •) 20, (- - -) 31.25, (- - •) 50, (- • -) 100, (— • —) 200, (—• • —) 312.5, and (— — —) 500 Hz.

$$\frac{1}{C_{total}} = \frac{1}{C_E} + \frac{1}{C_B} \tag{8}$$

where

$$C_E = \frac{\epsilon_0 \epsilon' P}{d_E} \quad \text{and} \quad C_B = \frac{\epsilon_0 \epsilon' P}{d_B}$$

P represents the area of E and B. The dipole contribution of the methylene spacer is negligible. C_{total} will depend on d_B because $1/C_E$ is a constant; therefore, the observed capacitance, C_{total}, has an inverse relationship with the side chain length (while other parameters are kept the same).

$\Delta\epsilon'(f)$ represents the difference in ϵ' between the low end and high end frequencies and is proportional to the effective number of dipoles involved in the relaxation. They all share the general feature that the magnitude decreases with temperature because of an increase in dipole fluctuation.[26]

Cop10/50% NBP showed a slightly higher $\Delta\epsilon'(f)$ than Cop11/50% NBP (volume effect or rigidity effect). Cop5/50% NBP showed the highest value due to the spacer effect. The trend in Cop10/50% NBP and Cop11/50% NBP suggests that the change is higher for a shorter

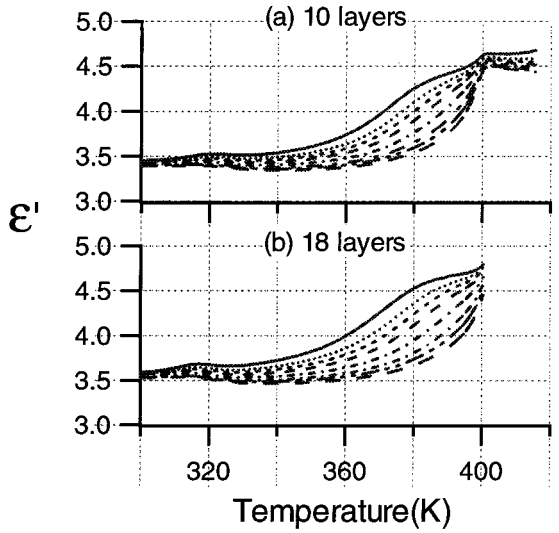

Figure 13. ϵ' of Cop11/50% NBP at 10 and 18 layers (first run): (—)10, (• • •) 20, (- - -) 31.25, (- - •) 50, (- • -) 100, (— • —) 200, (—• • —) 312.5, and (— — —) 500 Hz.

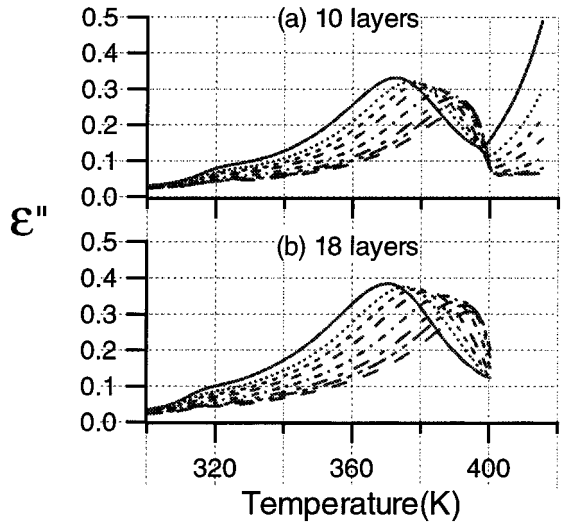

Figure 14. ϵ'' of Cop11/50% NBP at 10 and 18 layers (first run): (—)10, (• • •) 20, (- - -) 31.25, (- - •) 50, (- • -) 100, (— • —) 200, (—• • —) 312.5, and (— — —) 500 Hz.

spacer length, assuming they all relax in the same manner. The shorter spacer length is involved in a larger change in $\Delta\epsilon'(f)$ because of a smaller volume.

The broadening of the peak can be attributed to the cooperative nature of the relaxation. The β-relaxation, the relaxation prior to the K—LC transition, is interpreted as cooperative motions of the methoxy ethoxy biphenyl (MEMBP) and nitrobiphenyl (NBP) side chains. The nature of the cooperative motions was observed to be different between copolymers with long and short spacers. This is expected since the cooperative motions between MEMBP and NBP are imposed by chain connectivity, side chain length, and the polymeric backbone. These relaxations were observed in FTIR by Ou et al. in the same temperature range as an increase in CH_2 motion; however, an exact transition could not be identified.[21] The motion of CH_2 as a function of temperature was less in the second heating because of some structural rearrangement.

Effect of Thickness. The interaction between the first few layers with the substrate were expected to be different from the bulk. The analysis of the second harmonic generation (SHG) measurement of Cop11/50% NBP led to an interpretation that the dipoles in the first layer have a tilt angle of approximately 21° to the normal.[21]

Samples of Cop11/50% NBP with thicknesses of 10, 15, and 18 layers were studied (Figures 13 and 14). The anomalous peak is present in all the samples and disappears after sufficient crystalline heating.

The thickness was found to have no effect on the position of the anomalous peak. The $\epsilon'(T)$ and $\epsilon''(T)$ were qualitatively the same for the 10-, 15-, and 18-layer samples. The difference was the magnitude of $\epsilon''(T)$ in the 10-layer sample which was lower than that in the thicker samples. The activation energy is reduced as the number of layers increases; however, they still fall into the same range (Table 2 and Figure 15).

The difference is expected to be less as the sample becomes thicker because of the relative weighting of bulk and surface. The interpretation becomes more complicated as the oxide layer of the aluminum needs to be taken into consideration.[29] The oxide layer is limited to a very thin layer because of the limited

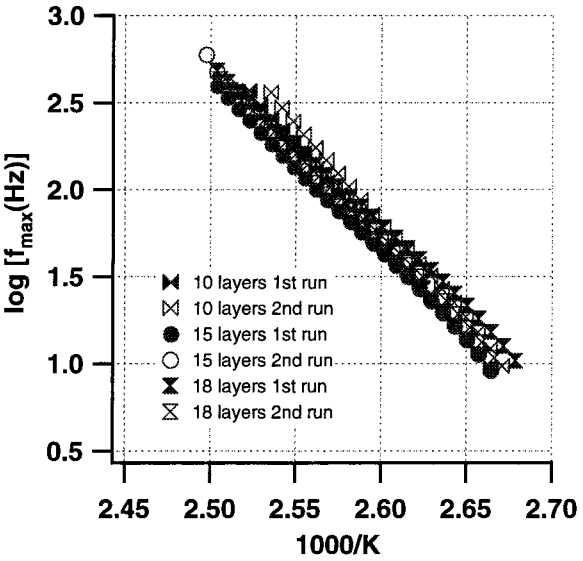

Figure 15. Plot of $\log[f_{max}(\text{Hz})]$ vs $1000/T$ of Cop11/50% NBP at 10, 15, and 18 layers.

permeation of the oxygen through the aluminum oxide layer.

The observed β-relaxation should not be effected by the oxide layer. The difference in the magnitude of all the observed parameters between Cop11/50% NBP 10 layers and the thicker sample must arise from the samples themselves. Therefore, it is reasonable to conclude that the first layer caused a difference in the effective material properties which is expected to be less as the film thickness increases.

Composition Effect. The dynamics of the film should be effected by the distribution/population of a particular group within the material. In this case, the homopolymer (H11MEMBP) and the copolymers (Cop11/20% NBP, Cop11/50% NBP, and Cop11/63% NBP) with spacer length 11 were investigated. The main difference among these materials is the ratio of NBP/MEMBP within the copolymer film.

H11MEMBP (Figures 16 and 17) showed a rather small peak superimposed on a broad reduction of $\epsilon'(T)$ between 320 and 360 K. These anomalous peaks disappeared after the samples were heated above 365 K

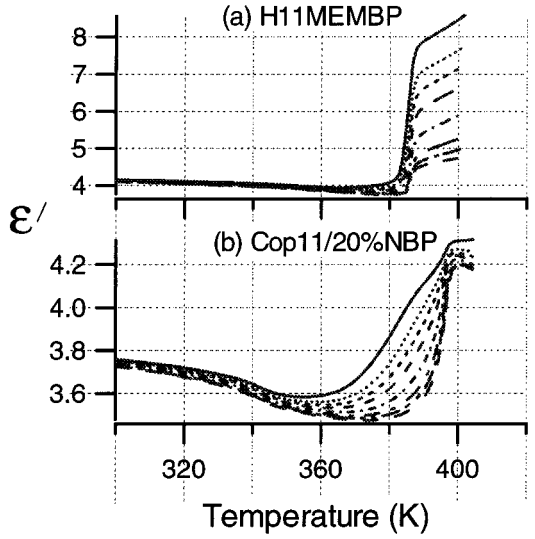

Figure 16. ϵ'' of H11MEMBP and Cop11/20% NBP first run: -(—)10, (• • •) 20, (- - -) 31.25, (- - •) 50, (- • -) 100, (— • —) 200, (—• • —) 312.5, and (— — —) 500 Hz.

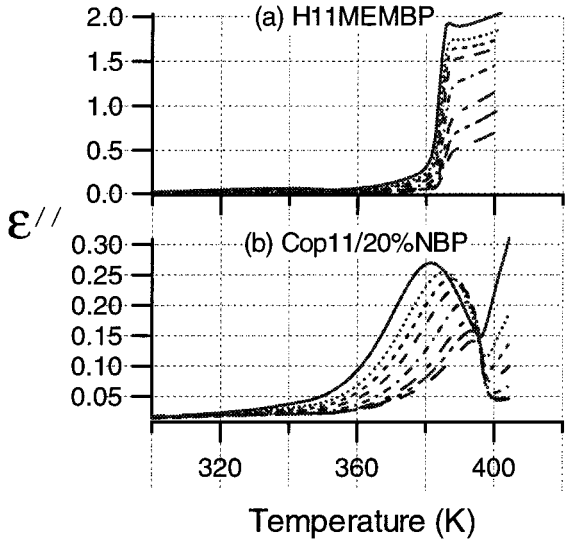

Figure 17. ϵ'' of H11MEMBP and Cop11/20% NBP first run: (—)10, (• • •) 20, (- - -) 31.25, (- - •) 50, (- • -) 100, (— • —) 200, (—• • —) 312.5, and (— — —) 500 Hz.

in H11MEMBP and Cop11/20% NBP and above 340 K in Cop11/50% NBP and Cop11/63% NBP. As stated previously, disappearance of the peaks is believed to be associated with the loss of some polarizable species from the film and/or some rearrangement.

Cop11/20% NBP showed a similar behavior to H11MEMBP at the low temperature where the small peak is superimposed on the broad reduction as a function of temperature.

Cop11/50% NBP showed a well-defined peak in both $\epsilon'(T)$ and $\epsilon''(T)$ between 310 and 330 K. The anomalous peak again disappeared after the sample was heated above 340 K.

Since copolymers with NBP higher than 50%, Cop11/63% NBP, do not spread at the gas−water interface as a true monolayer, a geometry-independent tan δ will be used for a comparison (Figures 18−20).[23] The anomalous process for Cop11/63% NBP was observed at approximately the same temperature range as in Cop11/50% NBP at a given frequency. The anomalous peak disappeared when the sample was heated above 340 K.

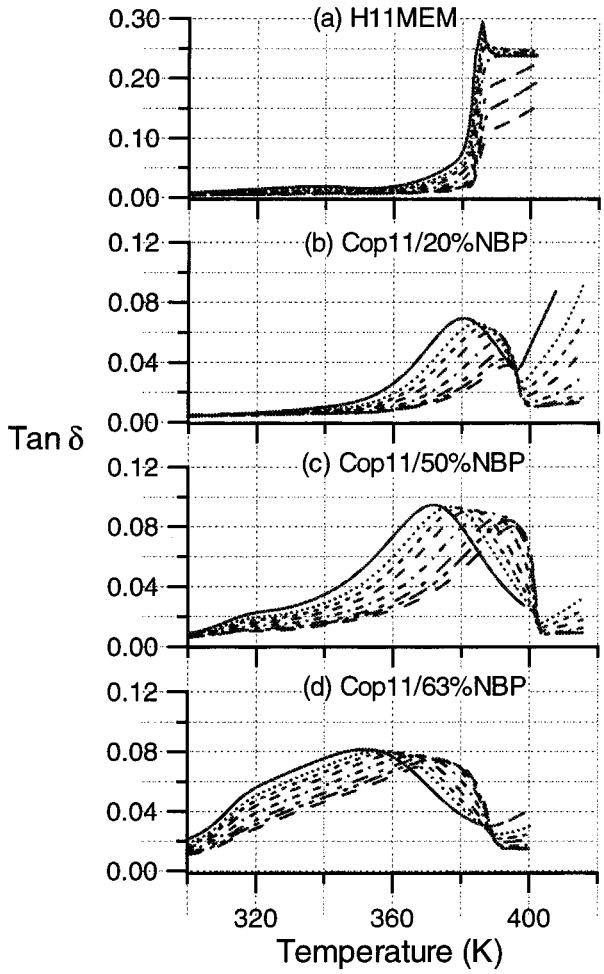

Figure 18. Tan δ of Cop11 system first run at various compositions: (—)10, (• • •) 20, (- - -) 31.25, (- - •) 50, (- • -) 100, (— • —) 200, (—• • —) 312.5, and (— — —) 500 Hz.

There are several possibilities that may contribute to this anomalous peak.[23] First, the peak may be due to water that was trapped at the MEM tail. It is reasonable since the MEM group is hydrophilic enough to include monolayer formation. Second is rearrangement within the film. This could arise from the breaking up of the NBP cluster and/or a changing of the orientation of the polar groups within film. At the gas−water interface the interaction is governed by the interaction between the headgroup and the water subphase as well as an interaction between the molecules. These local aggregations may cause the material in some areas to be NBP rich and behave differently from other areas. However, the size is limited to very small domains, and the response is limited. The majority of the response is still derived from the cooperative motion of MEMBP and NBP. Further experiments will be carried out by studying the pyroelectric effect and second harmonic generation as a function of temperature in an attempt to determine the nature of the anomalous peaks.

The relaxation of homopolymer NBP (H11NBP), in the bulk phase, is shown in Figure 22. At least two relaxations were observed. Note that the measurements were carried out at a temperature higher than the T_g of the homopolymer.

The magnitude of ϵ' at 300 K is H11MEMBP > Cop11/20% NBP > Cop11/50% NBP. At lower NBP composition, the main contribution arises from the polar MEM tail which contains ether, C−O, groups.

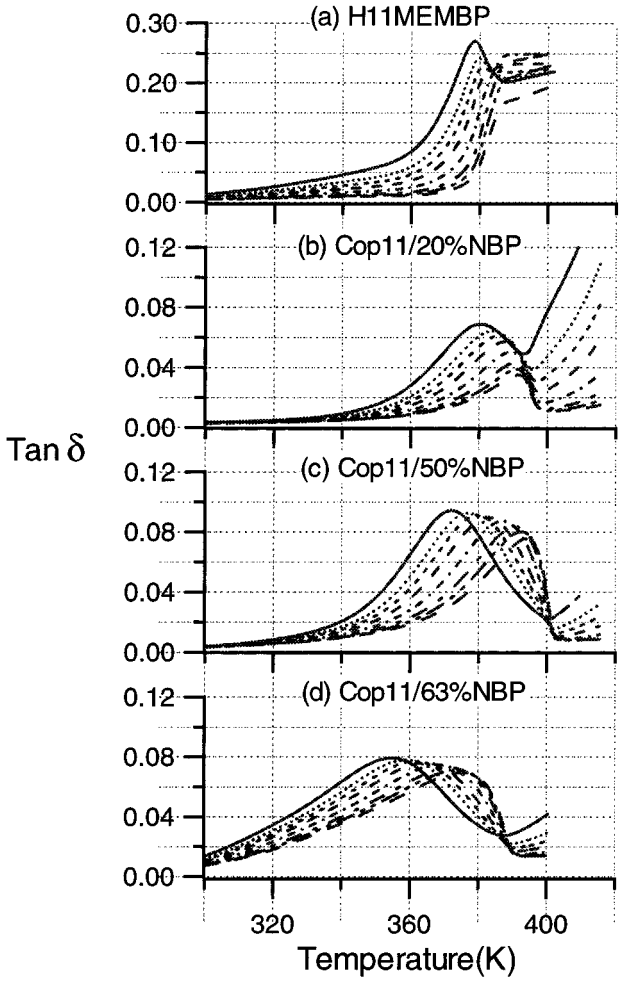

Figure 19. Tan δ of Cop11 system second run at various compositions: (—)10, (· · ·) 20, (- - -) 31.25, (- · -) 50, (- · -) 100, (— · —) 200, (—· · —) 312.5, and (— — —) 500 Hz.

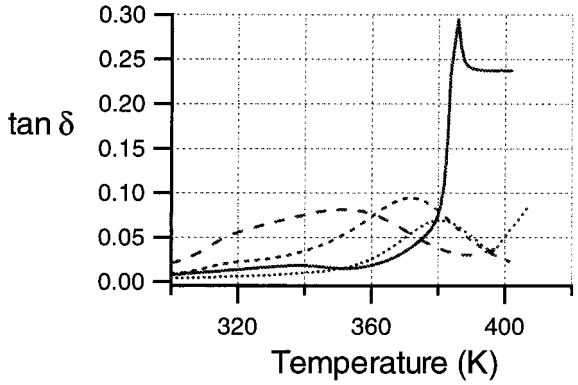

Figure 20. Plot of tan δ at 10 Hz of (a) (—) H11MEMBP, (b) (· · ·) Cop11/20% NBP, (c) (- - -) Cop11/50% NBP, and (d) (— — —) Cop11/63% NBP.

In the neighborhood of the K−LC phase transition, H11MEMBP shows a steep increase in both $\epsilon'(T)$ and $\epsilon''(T)$. The $\Delta\epsilon'(T)$ for H11MEMBP is very large which may be due to the proximity of the K−LC and LC−I transition. No β-relaxation is observed prior to the phase transition.

The onset of the β-relaxation is shifted to a lower temperature as the NBP is increased and eventually overlaps with the anomalous peak. This is probably due to a disrupted packing between the two side chains. The NBP homopolymer is rubbery at room temperature. The

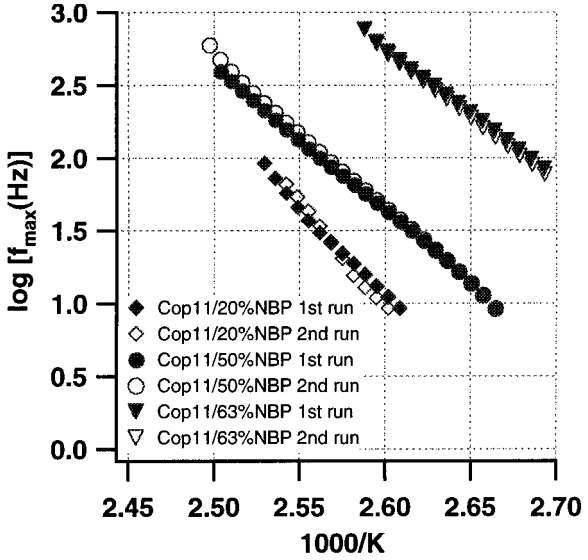

Figure 21. Plot of log [f_{max}(Hz)] vs 1000/T of Cop11 system (15 layers) at various copolymer compositions.

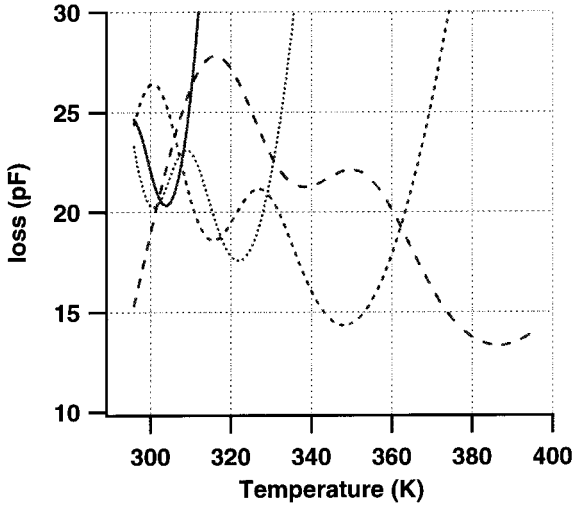

Figure 22. Loss of H11NBP vs temperature: (—) 10^2, (· · ·) 10^3, (- - -) 10^4, and (— — —)10^5 Hz.

activation energy for the β-relaxation is slightly different among Cop11/20% NBP, Cop11/50% NBP, and Cop11/63% NBP. The mismatch of the side chain packing is still observed as an increase in the loss at the low temperature because of the NBP group. The width factor, which is a function of copolymer composition, indicates that they are different in the nature of the cooperative motion of the dipole (Figure 23). The E_a of the β-relaxation is decreased as the amount of NBP is increased (Figure 21).

Effect of Chromophore Change. When nitrobiphenyl is replaced by the nitrostilbene, NSB, the magnitude of $\epsilon'(T)$ is slightly higher than in Cop11/50% NBP (Figures 24−26). The nitrostilbene possesses a higher hyperpolarizability. The observed ϵ' is effected by both the dipole moment and hyperpolarizability. Relative to NBP, the large change in $\epsilon'(T)$ and $\epsilon''(T)$ for NSB prior to the K−LC phase transition had taken place over a wider temperature range, which may indicate a difference in packing in the chromophore.

The magnitudes of $\epsilon'(T)$ and $\epsilon'(T)$ are about the same in both Cop11/50% NBP and Cop11/50% NSB, but $\Delta\epsilon''(f)$ of Cop11/50% NSB is higher than that of Cop11/50% NBP. The E_a is about the same for Cop11/50% NBP and

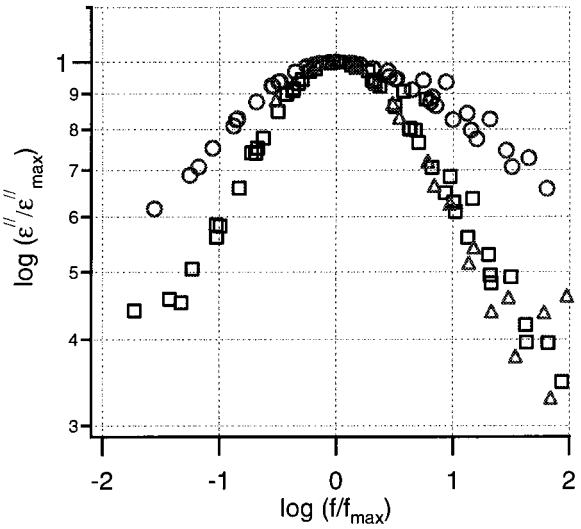

Figure 23. Universal plot for Cop11/20% NBP (△) from 385−395 K, Cop11/50% NBP (□) from 380−400 K, and Cop11/63%MBP (○) from 365−380 K.

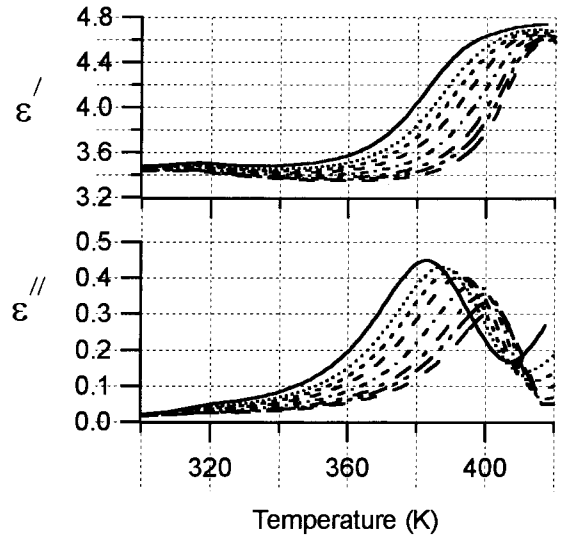

Figure 24. Plot of ϵ' and ϵ'' vs temperature of Cop11/50% NSB first run: (—)10, (· · ·) 20, (- - -) 31.25, (- - ·) 50, (- · -) 100, (— · —) 200, (—· · —) 312.5, and (— — —) 500 Hz.

Cop11/50% NSB as indicated in Figure 26 with comparisons listed in Table 2.

In both Cop11/50% NBP and Cop11/50% NSB samples, the MEMBP chain is terminated with a long flexible MEM group. To examine the effect of this chain on the anomalous peak, samples were prepared with OMe replacing the MEM chain. Judging from the co-area, the samples did not form a true monolayer. Along with the β-relaxation the samples showed the anomalous peak in the initial temperature scan which was not present in subsequent temperature cycles (Figures 24−26). The uptake of water should be less associated with the OMe group then the MEM group. Therefore, it is likely that the anomalous peak cannot be associated with the "melting" of the MEM group as well as the loss of water from the film, further strengthening the possibility of some rearrangement in the film, perhaps of the type suggested previously.[23]

Conclusion

1. Dielectric spectroscopy can be applied to study the dynamics of an ultrathin LB film. The method has excellent sensitivity in detecting the effect of the spacer length, copolymer composition, and the K−LC phase transition since sensitivity to the measured parameters is inversely proportional to the sample thickness.

2. A β-relaxation was observed in samples containing an NBP or NSB group. The NBP also acts as a packing mismatch in the copolymer and causes the β relaxation to broaden.

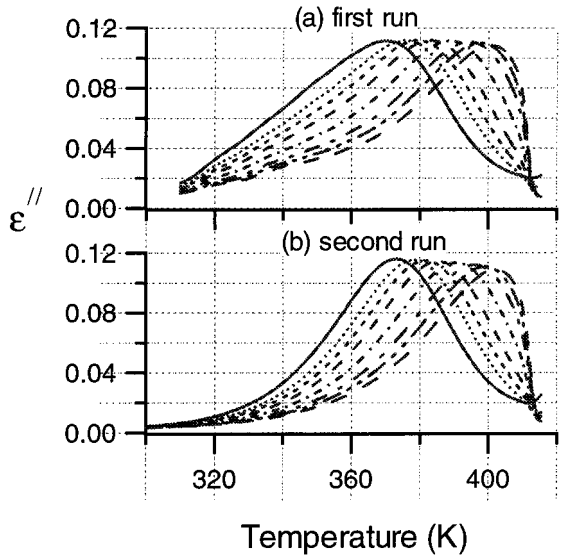

Figure 25. Tan δ of Cop11/50% OMe first and second run at (—)10, (· · ·) 20, (- - -) 31.25, (- - ·) 50, (- · -) 100, (— · —) 200, (—· · —) 312.5, and (— — —) 500 Hz.

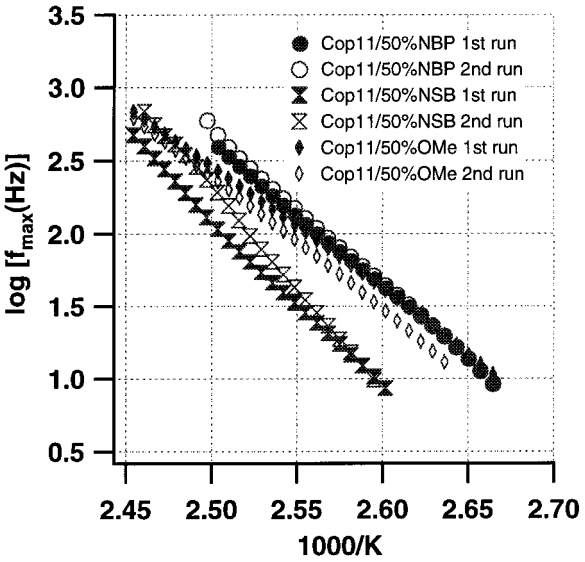

Figure 26. Plot of log[f_{max} (Hz)] vs 1000/T of Cop 11/50% NBP, Cop11/50% NSB, and Cop11/50% OMe (15 layers) first and second run.

Acknowledgment. This study has been supported by Advanced Liquid Crystalline Optical Materials (ALCOM), an NSF Science and Technology Center, under Contract DMR-89-20147.

References and Notes

(1) Ulman, A. In *An Introduction to Ultrathin Organic Films*; Academic Press: Boston, 1991.
(2) *2. Langmuir−Blodgett Films*; Robert, G., Ed.; Plenum Press: New York, 1990.
(3) (a) Swalen, J. D. *J. Mol. Electron.* **1986**, *2*, 155−181. (b) Swalen, J. D.; Allara, D. L.; Andrade, J. D.; Chandross, E.

A.; Garoff, S.; Israelachvili, J.; McCarthy, T. J.; Murray, R.; Pease, R. F.; Rabolt, J. F.; Wynne, K. J.; Yu, H. *Langmuir* **1987**, *3*, 932−950.
(4) Petty, M. C. In *An Introduction to Langmuir−Blodgett Films*; Cambridge University Press: New York, 1996.
(5) (a) Prasad, P. N.; Williams, D. J. In *Introduction to Nonlinear Optical Effects in Molecules and Polymers*; Wiley: New York, 1991. (b) William, D. J. In *Nonlinear Optical Properties of Organic Molecules and Crystals*; Chemla, D. S., Zyss, J., Eds.; Academic Press: Boston, 1987.
(6) *Characterization of Organic Thin Films*; Ulman, A., Ed.; Butterworth-Heinemann: Boston, 1995.
(7) (a) McCrum, N. G.; Read, B. E.; Williams, G. In *Anelastic and Dielectric Effects in Polymeric Solids*; Dover Publications: New York, 1991.
(8) Harrop, P. J. In *Dielectrics*; John Wiley and Sons: New York, 1972.
(9) Runt, J. P.; Fitzgerald, J. J. In *Dielectric Spectroscopy of Polymeric Materials, Fundamentals and Applications*; American Chemical Society: Washington, DC, 1997.
(10) Daniel, V. V. In *Dielectric Relaxation*; Academic Press: New York, 1967.
(11) (a) Jonscher, A. K. In *Dielectric Relaxation in Solids*; Chelsea Dielectrics Publishers: London, 1983. (b) Millany, H. M.; Jonscher, A. K. *Thin Solid Films* **1980**, *68*, 257−273. (c) Careem, M.; Jonscher, A. K. *Philos. Mag.* **1977**, *35*, 1489−1502. (d) Careem, M.; Jonscher, A. K.; Taiedy, F. *Philos. Mag.* **1977**, *35*, 1503−1508.
(12) Haws, C. M.; Clark, M. G.; Attard, G. S. In *Side Chain Liquid Crystal Polymers*; McArdle, C. B., Ed.; Chapman and Hall: New York, 1989; Chapter 7.
(13) Beevers, M. S. In *Siloxane Polymers*; Clarson, S. J., Semlyen, J. A., Eds.; EH PTR PH: Chapter 9, 1993.
(14) (a) Williams, G. *Polymer* **1994**, *35*, 1915−1922. (b) Nazemi, A.; Williams, G.; Attard, G. S.; Karaz, F. *Polym. Adv. Technol.* **1992**, *3*, 157−168.
(15) (a) Singal, C. M.; Gupta, S. K.; Kapil, A. K.; Srivastava, V. K. *J. Appl. Phys.* **1978**, *49*, 3402−3405. (b) Gupta, S. K.; Singal, C. M.; Srivastava, V. *J. Appl. Phys.* **1977**, *48*, 2583−2586.
(16) Marc, G.; Messier, J. *Thin Solids Films* **1980**, *68*, 275−288.
(17) Taylor, D. M.; Mahboubian-Jones, M. G. B. *Thin Solids Films* **1982**, *87*, 167−179.
(18) Tanguy, J. *Thin Solids Films* **1972**, *13*, 33−39.
(19) Honig, E. P. *Thin Solids Film* **1976**, *33*, 231−236.
(20) Nathoo, M. H. *Thin Solids Films* **1973**, *16*, 215−226.
(21) (a) Ou, S.; Percec, V.; Mann, J. A.; Lando, J. B.; Zhou, L.; Singer, K. D. *Macromolecules* **1993**, *26*, 7263−7273. (b) Ou, S. H.; Mann, J. A.; Lando, J. B.; Zhou, L.; Singer, K. D. *Appl. Phys. Lett.* **1992**, *61*, 2284−2286.
(22) Nguyen, D. M.; Mayer, T. M.; Hubbard, S. F.; Singer, K. D.; Mann, J. A.; Lando, J. B. *Macromolecules* **1997**, *30*, 6150−6157.
(23) Srikhirin, T.; Mann, J. A., Jr.; Lando, J. B. *J. Polym. Sci., Polym. Chem.* **1999**, *37*, 1057−1070.
(24) Zentel, R.; Strobl, G. R.; Ringsdorf, H. *Macromolecules* **1985**, *18*, 960−965.
(25) (a) Alig I.; Jarek, M.; Hellmann, G. P. *Macromolecules* **1998**, *31*, 2245−2251. (b) Alig, I.; Braun, D.; Jarek, M.; Hellmann, G. P. *Macromol. Symp.* **1995**, *90*, 173−194.
(26) Akins, R. B. Ph.D. Dissertation, Case Western Reserve University, Cleveland, OH, 1991.
(27) Zhong, Z. Ph.D. Dissertation, Case Western Reserve University, Cleveland, OH, 1993.
(28) Bevington, P. R.; Robinson, D. K. In *Data Reduction and Error Analysis for the Physical Sciences*, 2nd ed.; McGraw-Hill: Boston, 1992.
(29) (a) Shutt, J. D.; Rickert, S. E. *J. Mol. Electron.* **1988**, *4*, 201−205. (b) Shutt, J. D.; Batzel, D. A.; Sudiwala, R. V.; Rickert, S. E.; Kenney, M. E.; *Langmuir* **1988**, *4*, 1240−1247.

MA991437Y